Metallacyclopentatriene−Butadienyl Carbene Rearrangement in the Oxidative Coupling of Alkynes Mediated by $[RuCp(SbR_3)(CH_3CN)_2]^+$ (R = Ph, *n*-Bu)†

Eva Becker,‡ Kurt Mereiter,§ Michael Puchberger,⊥ Roland Schmid,‡ and Karl Kirchner*,‡

Institute of Applied Synthetic Chemistry, Institute of Chemical Technologies and Analytics, and Institute of Material Chemistry, Vienna University of Technology, Getreidemarkt 9, A-1060 Vienna, Austria

Received January 17, 2003

The oxidative coupling of alkynes is investigated as promoted by the half-sandwich compound $[RuCp(SbR_3)(CH_3CN)_2]PF_6$ (R = Ph, *n*-Bu). There are various ways by which the initially formed electrophilic metallacyclopentatriene complex rearranges to a stable product. In the case where the alkyne disposes of an α-alkyl substituent, intramolecular 1,2 hydrogen migration leads to a butadienyl carbene complex as obtained by using 2,8-decadiyne or $HC{\equiv}CCH_2R'$ (R′ = *n*-Pr, Ph, OH). A conceivable mechanism for this reaction sequence is established by means of DFT/B3LYP calculations. In line with experiment, the existence of two isomeric butadienyl carbene complexes is proposed. In the case of R′ = Ph and OH the butadienyl carbene is not the final product but rearranges to give η^3-allyl-vinyl and η^3-allyl-acyl complexes. In the absence of an α-alkyl substituent as for $HC{\equiv}CC_6H_9$, $HC{\equiv}CC_6H_{10}$-OH, and $HC{\equiv}CCMe_2OH$, η^3-butadienyl-vinyl complexes are formed. Finally, from the alkynes HC≡CPh, $HC{\equiv}CBu^t$, and $HC{\equiv}CSiMe_3$ no tractable materials are obtained.

Introduction

Recent studies of the interactions between the $[RuCp(ER_3)]^+$ moiety, derived from labile $[RuCp(ER_3)(CH_3CN)_2]PF_6$, and alkynes have revealed a subtle and diverse coordination chemistry.[1,2] Thus, depending on the ER_3 co-ligand, where E is a group 15 element, and the structure of the alkyne, a large variety of oxidative coupling products has been encountered such as allyl, butadienyl, allenyl, and vinylidene complexes. It would appear that there is a common initial step featured by the formation of a highly electrophilic cationic metallacyclopentatriene species[3] which is stabilized by subsequent rearrangement(s). The two main reaction schemes are (i) ligand migration, which gives initially allyl carbenes, and (ii) a 1,2 hydrogen shift resulting in butadienyl carbenes. Pathway (i) is favored if the ER_3 co-ligand is not too bulky and appreciably nucleophilic toward carbon. The alternative pathway (ii) is preferred if at least two conditions are met, namely, a weakly nucleophilic co-ligand as is the case for E = As and Sb and an alkyne with an α-alkyl substituent.

The present work is intended to investigate in some more detail the metallacyclopentatriene−butadienyl carbene conversion at $[RuCp(SbR_3)(CH_3CN)_2]PF_6$ (R = Ph (**1a**), *n*-Bu (**1b**)). In the preceding paper we used 2,8-decadiyne as the alkyne.[2] Here now we perform a labeling study by applying 2,8-decadiyne-d_6 to help elucidate the intimate mechanism of the 1,2 hydrogen shift. Furthermore we will use a range of terminal alkynes $HC{\equiv}CCH_2R'$, with and without α-alkyl substituents, to get some hints as to the reactivity of butadienyl carbene complexes, including their behavior toward bases. Finally the mechanistic considerations will be supported by DFT/B3LYP calculations.

Results and Discussion

Synthetic Aspects. As already described,[1,2] complexes **1a** and **1b** react with 2,8-decadiyne to give via a metallacyclopentatriene intermediate (**2**) the butadienyl carbenes **3a** and **3b** (Scheme 1). The involvement of a metallacylopentatriene intermediate on the pathway to butadienyl carbenes is evident from ^1H and $^{13}C\{^1H\}$ NMR spectroscopic studies. Thus, the resonances in the $^{13}C\{^1H\}$ NMR spectrum of $[RuCp(=C_2(CH_3)_2C_2(CH_2)_4)(SbPh_3)]^+$ (**2**) at 330.3 and 171.3 ppm can be associated with the C_α and C_β ring carbons, respectively.[2] The unusual downfield shifted resonances of the C_α carbon atoms is in agreement with an unsaturated bis-carbene

† Dedicated to Prof. John P. Hunt, a very respected friend and colleague, on the occasion of his 80th birthday.

* Corresponding author. E-mail: kkirch@mail.zserv.tuwien.ac.at.
‡ Institute of Applied Synthetic Chemistry.
§ Institute of Chemical Technologies and Analytics.
⊥ Institute of Material Chemistry.

(1) (a) Rüba, E.; Mereiter, K.; Schmid, R.; Kirchner, K. *Chem. Commun.* **2001**, 1996. (b) Rüba, E.; Mereiter, K.; Schmid, R.; Sapunov, V. N.; Kirchner, K.; Schottenberger, H.; Calhorda, M. J.; Veiros, L. F. *Chem. Eur. J.* **2002**, *8*, 3948.

(2) Becker, E.; Rüba, E.; Mereiter, K.; Schmid, R.; Kirchner, K. *Organometallics* **2001**, *20*, 3851.

(3) For metallacyclopentatriene complexes see: (a) Albers, M. O.; deWaal, D. J. A.; Liles, D. C.; Robinson, D. J.; Singleton, E.; Wiege, M. B. *J. Chem. Soc., Chem. Commun.* **1986**, 1680. (b) Gemel, C.; LaPensée, A.; Mauthner, K.; Mereiter, K.; Schmid, R.; Kirchner, K. *Monatsh. Chem.* **1997**, *128*, 1189. (c) Pu, L.; Hasegawa, T.; Parkin, S.; Taube, H. *J. Am. Chem. Soc.* **1992**, *114*, 2712. (d) Hirpo, W.; Curtis, M. D. *J. Am. Chem. Soc.* **1988**, *110*, 5218. (e) Kerschner, J. L.; Fanwick, P. E.; Rothwell, I. P. *J. Am. Chem. Soc.* **1988**, *110*, 8235. (f) Hessen, B.; Meetsma, A.; van Bolhuis, F.; Teuben, J. H.; Helgesson, G.; Jagner, S. *Organometallics* **1990**, *9*, 1925. (g) Ernst, C.; Walter, O.; Dinjus, E.; Arzberger, S.; Görls, H. *J. Prakt. Chem.* **1999**, *341*, 801.

10.1021/om030039n CCC: $25.00
Publication on Web 04/17/2003

Scheme 1

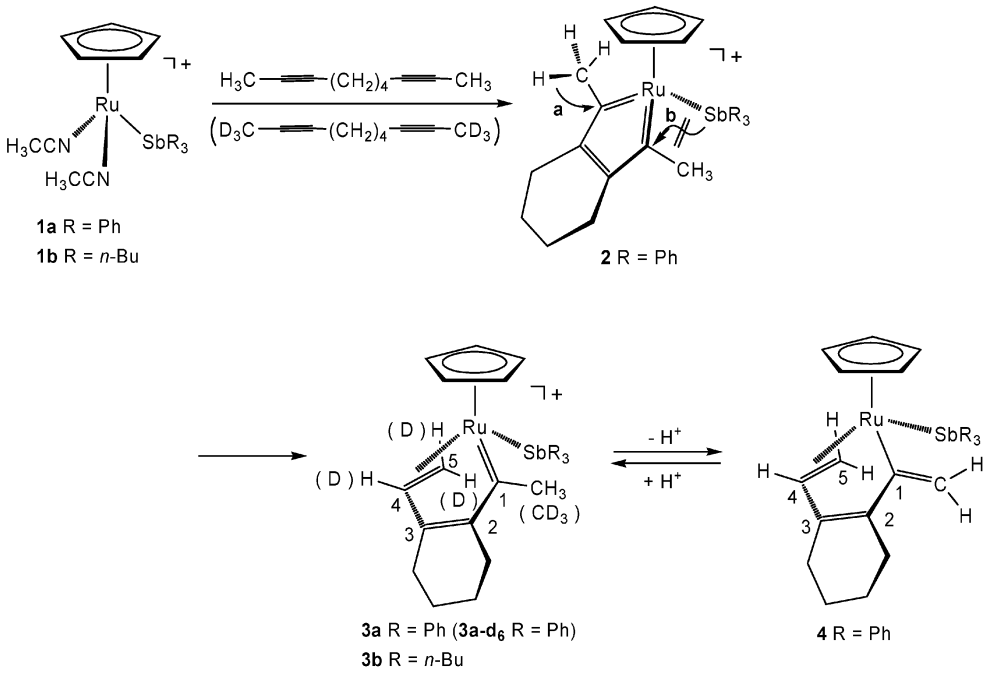

ligand. The analogous phosphine-based metallacyclopentatriene $[RuCp(=C_2(CH_3)_2C_2(CH_2)_4)(PCy_3)]^+$ also exhibits the characteristic resonances of the C_α and C_β ring carbons at 325.6 and 170.6 ppm, respectively[1a] (cf. the neutral metallacyclopentatriene $RuCp(=C_2(Ph)_2C_2H_2)$-Br, for which the respective resonances of the C_α and C_β atoms are found at 271.1 and 156.0 ppm[3a]). This conversion involves a net 1,2 hydrogen shift. To establish whether an intramolecular or intermolecular migration process is operative, we treat here **1a** with 2,8-decadiyne-d_6 in acetone, whereupon **3a**-d_6 was obtained quantitatively. The comparison of its ^{1}H NMR spectrum with that of **3a** obtained from 2,8-**1a** and 2,8-decadiyne acetone-d_6 shows that the resonances of the methyl substituent and the resonances of the $-CH=CH_2$ unit are absent. There is no indication that scrambling with hydrogen from the solvent occurred. Complementarily, the ^{2}H spectrum of **3a**-d_6 exhibits exclusively four resonances at 4.89−4.31 (D^a), 3.22−2.37 (D^c), 2.15 (CD_3), and 1.47−1.03 (D^b) ppm. In addition, a crossover study was conducted in which an equimolar mixture of 2,8-decadiyne and 2,8-decadiyne-d_6 was reacted with **1a** in acetone-d_6 at room temperature, revealing that only **3a** and **3a**-d_6 were formed. Accordingly, no scrambling of D was observed, and it is therefore reasonable to assume that hydrogen migration has taken place in an intramolecular fashion. On the basis of this competition experiment a large primary kinetic isotope effect of $k_H/k_D(25\ °C) = 10.0 \pm 0.5$ was observed, clearly showing that C−H (or C−D) bond cleavage is involved in the rate-determining step. The magnitude of this isotope effect would be consistent with a direct 1,2 hydrogen (or 1,2 deuterium) migration.

It may be noted that a 1,2 hydrogen shift is hitherto known only for electrophilic, typically cationic, alkyl carbenes such as $[FeCp(CO)_2(=C(CH_3)_2)]^+$ and related species.[4] Taube and co-workers reported for the first time the conversion of the dicationic osmacyclopentatriene complex $[Os(en)_2(=C_2(CH_3)_2C_2(CH_3)_2)]^{2+}$ to a butadienyl carbene in the presence of *tert*-butylamine, a process clearly related to our findings.[5]

The reactivity of **3a** has been tested by treating it with bases. As a result, NEt_3 or *n*-BuLi leads to deprotonation of one methyl substituent to yield the neutral complex $RuCp(-C=CH_2)C(CH_2)_4C$-η^2-$CH=CH_2)(SbPh_3)$ (**4**). This reaction is particularly clean if a solution of **3a** in CH_2Cl_2 is chromatographed over basic Al_2O_3, affording **4** in 68% isolated yield (Scheme 1). With **3b**, on the other hand, no reaction took place. Product **4** was characterized by a combination of elemental analysis and ^{1}H and $^{13}C\{^1H\}$ NMR spectroscopies. Characteristic solution ^{1}H NMR spectroscopic data include two doublets at 5.46 (H^b) and 4.68 (H^a) ppm with a coupling constant $^2J_{HH} = 2.4$ Hz assignable to the hydrogen atoms of the vinyl $-C=CH_2$ unit and two doublets and one triplet a 4.79 (H^d), 2.73 (H^e), and 4.62 (H^c) ppm with a *cis* and *trans* coupling constant $^3J_{HH} = 8.9$ Hz assignable to the hydrogen atoms of the butadienyl moiety. The $^{13}C\{^1H\}$ NMR signals appearing at 161.0, 62.6, and 31.5 ppm are assignable to the vinyl carbon atom C^1 and the coordinated olefinic carbon atoms C^5 and C^6, respectively. All other resonances are unremarkable.

It is worth noting that the formation of **4** is reversible. In fact, addition of H_2SO_4 leads to a clean back-transformation to **3a**. If D_2SO_4 is used instead, the isotopomer **3a**-d_6 is obtained. That is, quantitative scrambling of D into the methyl substituent has taken place. This behavior can be interpreted in terms of an equilibrium reaction occurring between **3a** and **4**.

The structural identity of **4** was established by X-ray crystallography. The result depicted in Figure 1 shows

(4) For carbene to olefin conversions see: (a) Casey, C. P.; Miles, W. H.; Tukada, H. *J. Am. Chem. Soc.* **1985**, *107*, 2924. (b) Bodnar, T.; Cutler, A. R. *J. Organomet. Chem.* **1981**, *213*, C13. (c) Fischer, E. O.; Held, W. *J. Organomet. Chem.* **1976**, *112*, C59.

(5) Pu, L.; Hasegawa, T.; Parkin, S.; Taube, H. *J. Am. Chem. Soc.* **1992**, *114*, 7609.

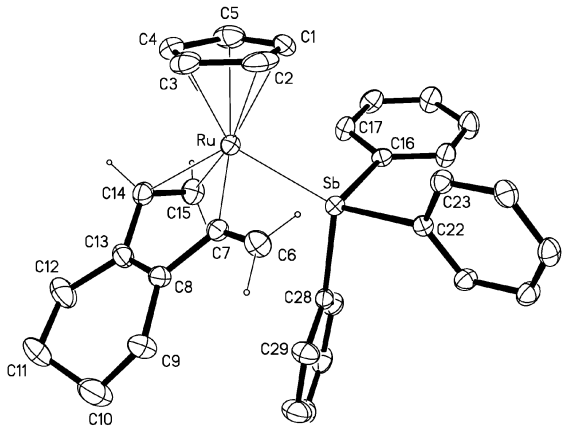

Figure 1. Structural view of [RuCp(−C═CH_2)C$(CH_2)_4$C-η^2-CH═CH_2)($SbPh_3$)] (**4**) showing 20% thermal ellipsoids (H atoms outside the triene system C6−7−8−13−14−15 omitted for clarity). Selected bond lengths (Å) and angles (deg): Ru−C(1−5)$_{av}$ 2.209(5), Ru−C(7) 2.092(4), Ru−C(14) 2.169(5), Ru−C(15) 2.188(5), Ru−Sb 2.529(1), C(6)−C(7) 1.346(6), C(7)−C(8) 1.459(6), C(8)−C(13) 1.328(6), C(13)−C(14) 1.482 (6), C(14)−C(15) 1.393(7), C(7)−Ru−C(14) 78.4(1), C(7)−C(8)−C(13)−C(14) 2.7(6).

a three-legged piano stool conformation with $SbPh_3$, with the two C═C bonds butadienyl moiety, and the vinyl carbon atom as the legs. The Ru−C(7) bond distance of 2.092(4) Å is in line with a metal carbon single bond. The Ru−C(14) and Ru−C(15) bond distances are 2.169(5) and 2.188(5) Å, respectively. The butadienyl C−C bonds C(8)−C(13), C(13)−C(14), and C(14)−C(15) show the expected short−long−short pattern (1.328(6), 1.482(6), and 1.393(7) Å, in the same order). The Ru−Sb bond length of 2.529(1) Å may be compared with the 2.575(1) Å in **3a**.

We now turn to the reaction of **1** with various terminal alkynes HC≡CCH_2R′ noting a dramatic substituent effect of R′ on the outcome. With R′ = *n*-Pr, Ph, the same result was obtained as with 2,8-decadiyne, giving the butadienyl carbenes **3c**−**e**. Interestingly, the structure of **3c** contains the butadienyl moiety in a distorted *s-trans* conformation rather than distorted *s-cis* as found in **3a**. The solid-state structure of **3c** is depicted in Figure 2 with important bond distances reported in the caption. Overall, the structure is similar to that of **3a**, i.e., a typical three-legged piano stool conformation with $SbPh_3$, with the two C═C bonds of the butadienyl moiety and the carbene carbon atom as the legs. The most notable feature is the short Ru−C(6) bond distance of 1.908(6) Å, reflecting a metal carbon double bond. The Ru−C(13) and Ru−C(14) bond distances are 2.260(5) and 2.188(8) Å, respectively. Furthermore, the butadienyl C−C bonds C(7)−C(12), C(12)−C(13), and C(13)−C(14) again show the expected short−long−short pattern of 1.346(8), 1.462(8), and 1.422(8) Å, respectively. Compound **3c** crystallizes also as as the acetone solvate **3c**·$(CH_3)_2CO$, which agrees in the inner part of the Ru complex very well with its unsolvated counterpart but differs in the conformations of both alkyl side chains (C(8)−C(11) and C(15)−C17)). Structural data of this compound have been deposited under CCDC-201214.

When R′ = Ph and OH, the butadienyl carbene complexes initially formed are not the final products but undergo further rearrangements giving η^3-allyl-vinyl

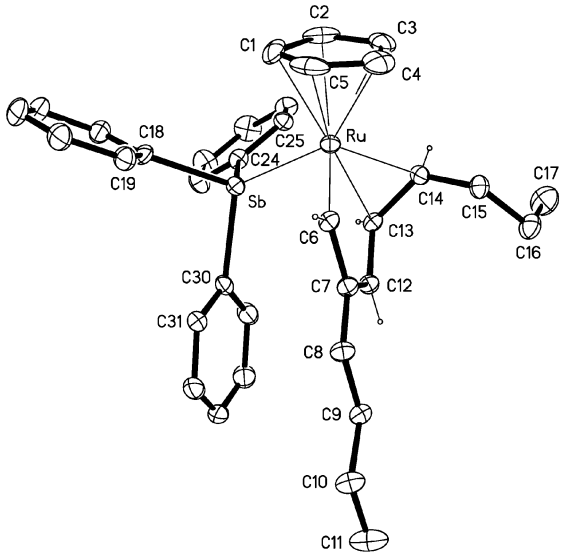

Figure 2. Structural view of [RuCp(═CHC(*n*-Bu)CH-η^2-CH═CH-*n*-Pr)($SbPh_3$)]PF_6 (**3c**) showing 20% thermal ellipsoids (H atoms outside the butadienyl carbene system and PF_6^- omitted for clarity). Selected bond lengths (Å) and angles (deg): Ru−C(1−5)$_{av}$ 2.239(8), Ru−C(6) 1.908(6), Ru−C(13) 2.260(5), Ru−C(14) 2.188(6), Ru−Sb 2.567(1), C(6)−C(7) 1.439(8), C(7)−C(12) 1.346(8), C(12)−C(13) 1.462(8), C(13)−C(14) 1.422(8), C(6)−Ru−C(13) 76.7(2), C(6)−C(7)−C(12)−C(13) 2.2(8).

and η^3-allyl-acyl complexes of the types [RuCp(η^3-$CH_2C(CH_2Ph)CH$-η^1-C═CH−Ph)(SbR_3)]PF_6 (**5a**,**b**)[2] and [RuCp(η^3-CH_2CCH_2−CH═CH-η^1-CO)(SbR_3)]PF_6 (**6a**,**b**), respectively (Scheme 2). The only exception is when HC≡CCH_2Ph is reacted with **1a**, where [RuCp(═CHC-(CH_2Ph)CH-η^2-CH═CH−Ph)($SbPh_3$)]PF_6 (**3d**) was isolated and characterized. Crystals grown from **5a** in acetone showed two different types, which, from single-crystal X-ray crystallographic analysis, turned out to be the acetone solvate **5a**·$(CH_3)_2CO$ and the ansolvate **5a**′. Both kinds of crystals were obtained by diffusion of Et_2O into acetone solutions at room temperature, giving at first the unstable solvate and on prolonged standing the stable ansolvate. The ORTEP plots are depicted in Figures 3 and 4 along with some selected bond distances and angles. Accordingly, while both possess a type of "three-legged piano stool" molecular structure, with $SbPh_3$, the three carbon atoms of the η^3-allyl moiety, and the vinyl carbon atom as the legs, they differ stereochemically. In **5a**·$(CH_3)_2CO$, the phenyl substituent of the vinyl unit is *cis* to the allyl moiety, in contrast to *trans* in **5a**′.

In the allyl vinyl system of **5a**′ all four carbon atoms of the C_{1-4} chain are bonded to the RuCp fragment. The C_{1-4} chain is nearly planar, with a torsion angle of 9.6(6)°. The Ru−C(9) distance is 2.123(4) Å, typical of a Ru−C vinyl single bond. The allyl moiety is bonded asymmetrically to the metal center with the Ru−C bonds to the terminal allyl carbon atoms C(6) and C(8) (2.223(4) and 2.191(4) Å, respectively) being longer than the Ru−C bond to the central allyl carbon atom C(7) (2.187(4) Å). The C−C distances within the allyl vinyl moiety are relatively uniform. The C(6)−C(7), C(7)−C(8), and C(8)−C(9) bond distances are 1.412(6), 1.409(6), and 1.416(6) Å, respectively, while the C(9)−C(10)

Scheme 2

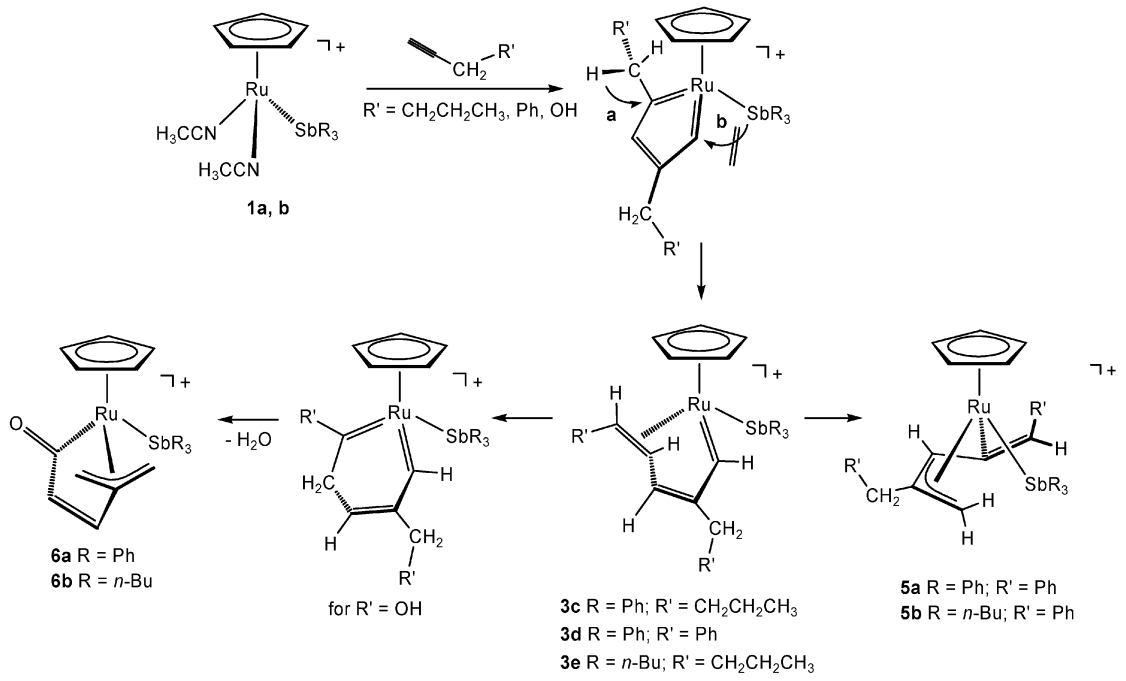

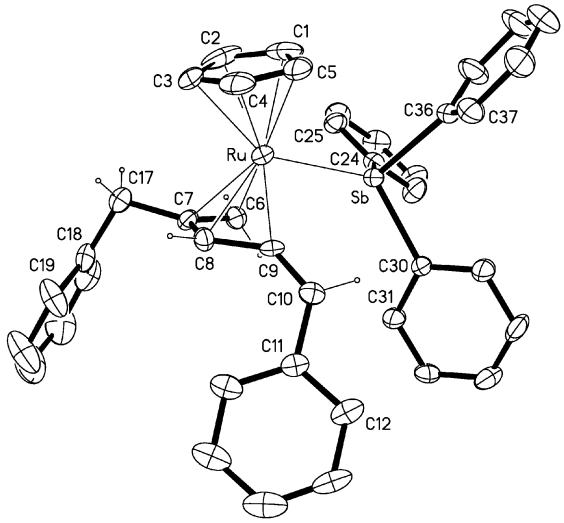

Figure 3. Structural view of *cis*-[RuCp(η^3-$CH_2C(CH_2Ph)$-CH-η^1-$C{=}CH{-}Ph)(SbPh_3)]PF_6{\cdot}(CH_3)_2CO$ (**5a**$\cdot(CH_3)_2CO$) showing 20% thermal ellipsoids (aromatic H atoms, PF_6^-, and $(CH_3)_2CO$ omitted for clarity). Selected bond lengths (Å) and angles (deg): Ru−C(1−5)$_{av}$ 2.200(10), Ru−C(6) 2.232(8), Ru−C(7) 2.184(8), Ru−C(8) 2.164(8), Ru−C(9) 2.086(8), Ru−Sb 2.575(1), C(6)−C(7) 1.398(11), C(7)−C(8) 1.436(11), C(8)−C(9) 1.407 (11), C(9)−C(10) 1.301(10), C(8)−C(9)−C(10)−C(11) 10.1(17).

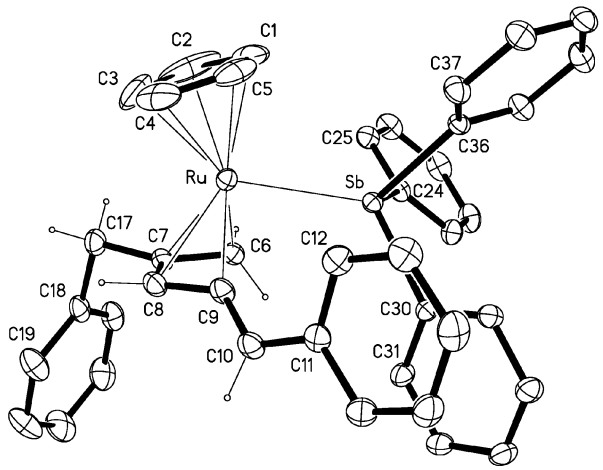

Figure 4. Structural view of *trans*-[RuCp(η^3-$CH_2C(CH_2$-$Ph)CH$-η^1-$C{=}CH{-}Ph)(SbPh_3)]PF_6$ (**5a′**) showing 20% thermal ellipsoids (aromatic H atoms and PF_6^- omitted for clarity). Selected bond lengths (Å) and angles (deg): Ru−C(1−5)$_{av}$ 2.183(8), Ru−C(6) 2.223(4), Ru−C(7) 2.187(4), Ru−C(8) 2.191(4), Ru−C(9) 2.123(4), Ru−Sb 2.599(1), C(6)−C(7) 1.412(6), C(7)−C(8) 1.409(6), C(8)−C(9) 1.416 (6), C(9)−C(10) 1.329(6), C(8)−C(9)−C(10)−C(11) −162.1(5).

distance is 1.329(6) Å, typical of a C−C double bond. The bond distances in **5a**$\cdot(CH_3)_2CO$ are very similar.

Complexes **6a** and **6b** are air-stable compounds. Support for the formulations comes from elemental analysis as well as from ^1H, $^{13}C\{^1H\}$ NMR and IR spectroscopy. The carbonyl stretching frequency of the acyl moiety in **6a** is observed at 1688 cm^{-1}. In the ^1H NMR spectrum of **6a** the Cp ring is found as a singlet at 5.81 ppm. The allyl moiety exhibits signals in the range 4.22−4.27 (2H, H^{5a}, H^{6a}), 4.21 (1H, H^{6s}), and 4.02 (1H, H^{5s}). The hydrogen atoms of the noncoordinated double bond display two characteristic doublets centered at 7.36 (H^3) and 7.36 (H^2) ppm with the coupling constant $^3J_{HH} = 6.8$ Hz. In the $^{13}C\{^1H\}$ NMR spectrum the acyl carbon atom is revealed by a characteristic singlet at 234.9 ppm, while the carbon atoms of the olefin unit are observed at 150.0 and 147.8 ppm, assignable to C^3 and C^2, respectively. The three allyl carbons appear as signals at 119.4, 68.0, and 44.5 ppm, assignable to C^4, C^5, and C^6, respectively. The Cp ligand shows a singlet at 93.5 ppm. The NMR spectra of **6b** are analogous. In the absence of crystals of **6a** and **6b** suitable for a single-crystal X-ray diffraction study, the structural assignment has been achieved by means of ^1H and ^{13}C NMR GIAO calculations based on the optimum DFT/B3LYP model of [RuCp(η^3-CH_2CCH_2-

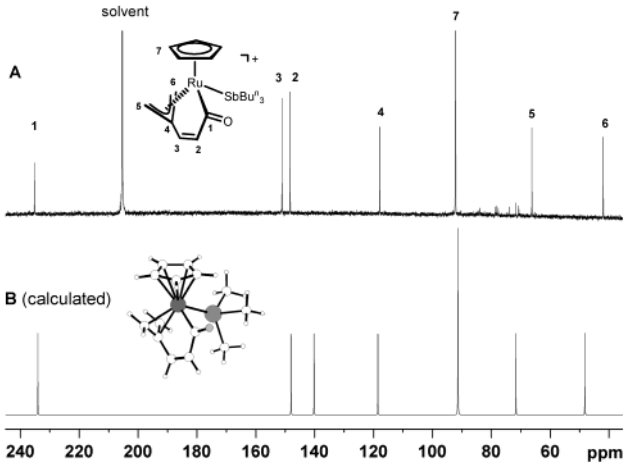

Figure 5. Experimental and calculated (DFT/B3LPY-GIAO) ^{13}C chemical shifts δ (in ppm relative to TMS) for $[RuCp(\eta^3\text{-}CH_2CCH_2{-}CH{=}CH\text{-}\eta^1\text{-}CO)(SbBu^n{}_3)]PF_6$ (**6b**) (spectrum A, solvent = acetone-d_6) and the DFT optimized model $[RuCp(\eta^3\text{-}CH_2CCH_2{-}CH{=}CH\text{-}\eta^1\text{-}CO)(SbMe_3)]^+$ (spectrum B), respectively (signals of $SbBu^n{}_3$ and $SbMe_3$ carbon atoms have been omitted for clarity).

$CH{=}CH\text{-}\eta^1\text{-}CO)(SbMe_3)]^+$. The calculated NMR spectra are in excellent agreement with the experimental values (see Experimental Section). In Figure 5 is compared the ^{13}C NMR spectrum of **6a** with that of the model complex $[RuCp(\eta^3\text{-}CH_2CCH_2CH{=}CH\text{-}\eta^1\text{-}CO)(SbMe_3)]^+$.

The actual mechanism for the formation of **6** remains unclear, since ^1H NMR monitoring of the reaction of **1** with propargylic alcohol at low temperatures did not reveal any intermediates. That is, only the disappearance of **1** and the quantitative formation **6** is observed. Notwithstanding this, a conceivable intermediate might be a hydroxycarbene complex[6] as result of an olefin-to-carbene rearrangement involving a 1,2 hydrogen shift from a butadienyl carbene (Scheme 2). It is well known indeed that the conversion of an activated olefin into a heteroatom-stabilized carbene is a thermodynamically favorable process.[7] During the reaction water is liberated, as detected by ^1H NMR spectroscopy.

The alkynes utilized so far contain an α-alkyl substituent capable of facile 1,2 hydrogen shift. In the following we also take other ones lacking α-C−H bonds, namely, $HC{\equiv}CC_6H_9$ and the propargylic alcohols $HC{\equiv}CC_6H_{10}OH$ and $HC{\equiv}CCMe_2OH$. In these three cases η^3-butadienyl-vinyl complexes are formed, as presented in Scheme 3. Thus with **1b** the compounds $[RuCp(\eta^1\text{-}CHC(C_6H_9)CH{=}(\eta^3\text{-}CC(CH_2)_4CH)(SbBu^n{}_3)]PF_6$ (**7b**), $[RuCp(\eta^1\text{-}CHC(C_6H_{10}OH)CH{=}(\eta^3\text{-}CC(CH_2)_4CH)(SbBu^n{}_3)]PF_6$ (**8**), and $[RuCp(\eta^1\text{-}CHC(Me)_2OHCH{=}(\eta^3\text{-}CC(Me)CH_2)(SbR_3)]PF_6$ (**9**) are obtained. $HC{\equiv}CC_6H_9$ was also reacted with **1a**, resulting in $[RuCp(\eta^1\text{-}CHC(C_6H_9)CH{=}(\eta^3\text{-}CC(CH_2)_4CH)(SbPh_3)]PF_6$ (**7a**).

All of these are air-stable compounds and were identified by a combination of ^1H and $^{13}C\{^1H\}$ NMR spectroscopy and elemental analysis. Since the overall spectroscopic features are very similar, we describe only those of **7a**. Characteristic signals of the ^1H NMR spectrum include two doublets centered at 8.10 and 6.84 ppm ($^4J_{HH}$ = 3.5 Hz) assignable to H^4 and H^6, respectively. In the $^{13}C\{^1H\}$ NMR spectrum the η^3-butadienyl unit is recognized by resonances at 197.4, 133.9, 94.1, and 66.4 ppm, assignable to C^3, C^4, C^2, and C^1, respectively.[8] Furthermore, the η^1-vinyl unit exhibits two signals at 165.5 and 119.6 ppm, assignable to C^5 and C^6, respectively.

Scheme 3

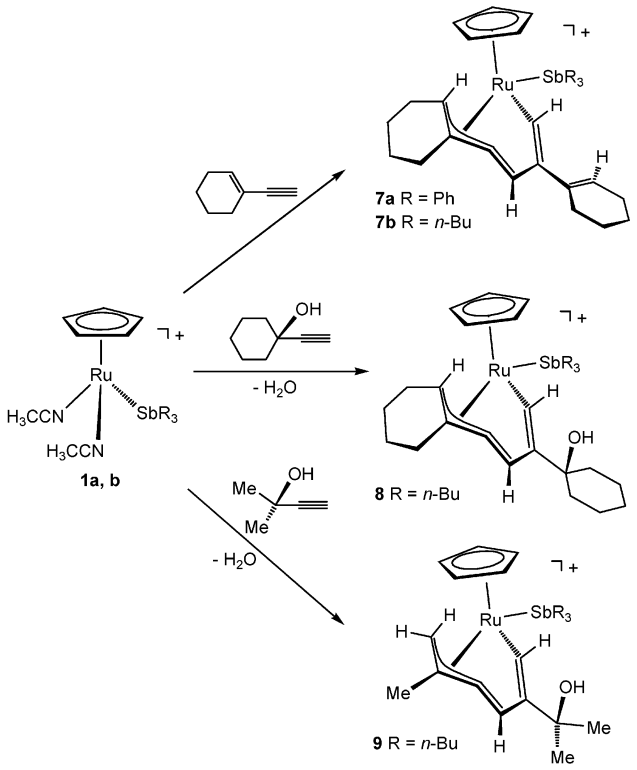

Finally, the interaction of the alkynes HC≡CPh, $HC{\equiv}CBu^t$, and $HC{\equiv}CSiMe_3$ with **1** did not result in any tractable materials. In these particular cases, as it would appear, no suitable reaction path is accessible to stabilize the initial metallacyclopentatriene intermediate.

Mechanistic Aspects. A conceivable pathway for the reaction of the model bisacetonitrile complex $[RuCp(SbH_3)(NCH)_2]^+$ (**A**) with the alkynes HC≡CH and $HC{\equiv}CCH_3$ used as model substrates is shown in Figure 6 based on DFT/B3LYP calculations using Gaussian98 (energy in kcal/mol).

The reliability of the computational method (details in Experimental Section) is supported by the good agreement between the calculated geometries of the two isomeric butadienyl carbene complexes **E** and **G** with the X-ray structures for the related complexes **3a** and **3c** despite the absence of substituents in the model. The

(6) Casey, C. P.; Czerwinski, C. J.; Fusie, K. A.; Hayashi, R. K. *J. Am. Chem. Soc.* **1997**, *119*, 3971, and references therein.

(7) (a) Coalter, J. N.; Spivak, G. J.; Gerard, H.; Clot, E.; Davidson, E. R.; Eisenstein, O.; Caulton, K. G. *J. Am. Chem. Soc.* **1998**, *120*, 9388. (b) Coalter, J. N.; Bollinger, J. C.; Huffman, J. C.; Zwanziger, U. W.; Caulton, K. G.; Davidson, E. R.; Gerard, H.; Clot, E.; Eisenstein, O. *New J. Chem.* **2000**, *24*, 9. (c) Slugovc, C.; Mereiter, K.; Schmid, R.; Kirchner, K. *Organometallics* **1998**, *17*, 827. (d) Heinekey, D. M.; Radzewich, C. E. *Organometallics* **1998**, *17*, 51.

(8) For η^3-butadienyl complexes see: (a) Slugovc, C.; Mereiter, K.; Schmid, R.; Kirchner, K. *Eur. J. Inorg. Chem.* **1999**, *1141*, 1. (b) Yi, C. S.; Liu, N.; Rheingold, A. L.; Liable-Sands, L. M. *Organometallics* **1997**, *16*, 3910. (c) Werner, H.; Wiedmann, R.; Steinert, P.; Wolf, J. *Chem. Eur. J.* **1997**, *3*, 127. (d) Bruce, M. I.; Duffy, D. N.; Liddell, M. J.; Tiekink, E. R. T.; Nicholson, B. K. *Organometallics* **1992**, *11*, 1527. (e) Bruce, M. I.; Hambly, T. W.; Liddell, M. J.; Snow, M. R.; Swincer, A. G.; Tiekink, E. R. T. *Organometallics* **1990**, *9*, 96.

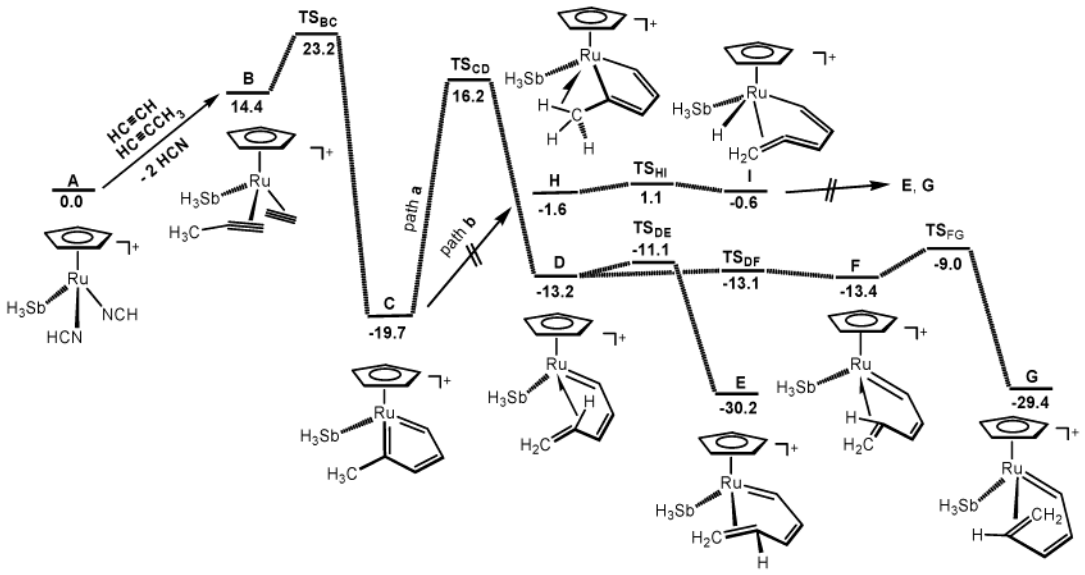

Figure 6. Profile of the B3LYP potential energy surfaces (in kcal/mol) for the conversion of **A** to the two isomeric butadienyl carbenes **E** and **G**.

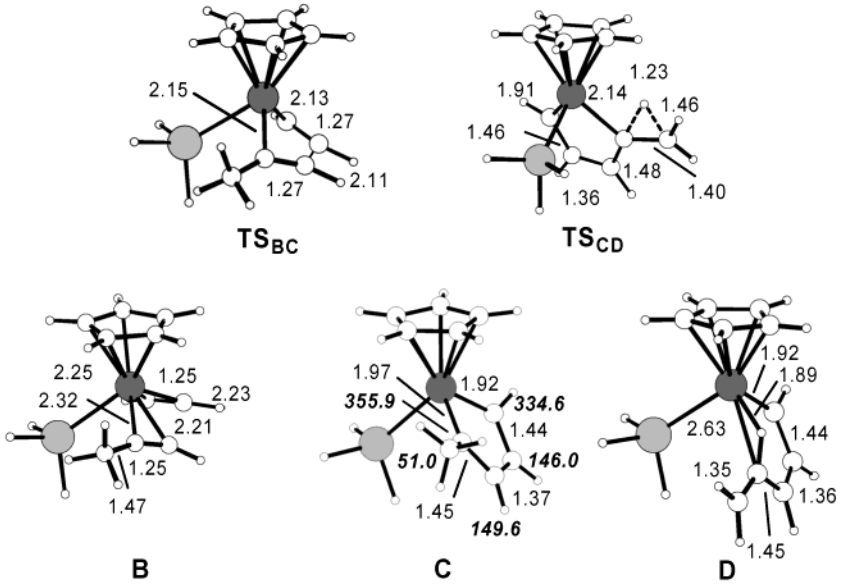

Figure 7. Optimized B3LYP geometries of the equilibrium structures and transition states **B**, **C**, **D**, $\mathbf{TS_{BC}}$, and $\mathbf{TS_{CD}}$ (distances in Å) and calculated (DFT-GIAO) ^{13}C chemical shifts δ (in ppm relative to TMS) for **C** (italic)

detailed structures of the entities **B**−**G** and the corresponding transition states $\mathbf{TS_{BC}}$−$\mathbf{TS_{FG}}$ are displayed in Figures 7 and 8.

The overall reaction from **A** to **E** and **G** is exothermic by −30.2 and −29.4 kcal/mol, respectively. In the initial step the ligated acetonitrile molecules are replaced by the acetylenes to give the bis-acetylene complex **B**. Such processes, as is known from experiment, proceed by a dissociative mechanism,[9] whereas the associative alternative needing concomitant $\eta^5 \rightarrow \eta^3$ ring slippage to preserve the 18-electron count can be ruled out. Note that the overall substitution reaction **A** + 2 HC≡CH → **B** + 2HCN is endothermic by 14.4 kcal/mol. Oxidative coupling of the acetylene ligands in **B** brings us in a symmetry-allowed process to the coordinatively saturated metallacyclopentatriene **C**. Location of the transition state $\mathbf{TS_{BC}}$ revealed a moderate activation barrier of 8.8 kcal/mol. The formation of **C** is strongly exothermic, releasing 34.1 kcal/mol. In this reaction step a new carbon−carbon bond starts to form, noting a C···C distance decrease from 2.73 in **B** to 2.11 in $\mathbf{TS_{BC}}$, to reach 1.37 Å in species **C**, characteristic of a C=C bond. Simultaneously the two acetylene ligands have to reorient themselves, so that two of the Ru−C bonds become stronger (distances decrease from 2.326, 2.25 (**B**), via 2.15, 2.13 ($\mathbf{TS_{BC}}$) to 1.92, 1.97 Å (**C**), and the other two weaker. These changes occur smoothly, with the transition state occupying an intermediate position somewhat closer to the bisacetylene complex than to the metallacycle. Note that the C_α−C_β distances are still rather short, exhibiting a triple-bond character (1.27 and 1.27 compared to 1.25 Å in the starting structure **B**), while C_β−$C_{\beta'}$ is still away from a bonding distance (2.11 Å). The calculated structure of **C** compares well with the

(9) Luginbühl, W.; Zbinden, P.; Pittet, P. A.; Armbruster, T.; Bürgi, H.-B.; Merbach, A. E.; Ludi, A. *Inorg. Chem.* **1991**, *30*, 2350.

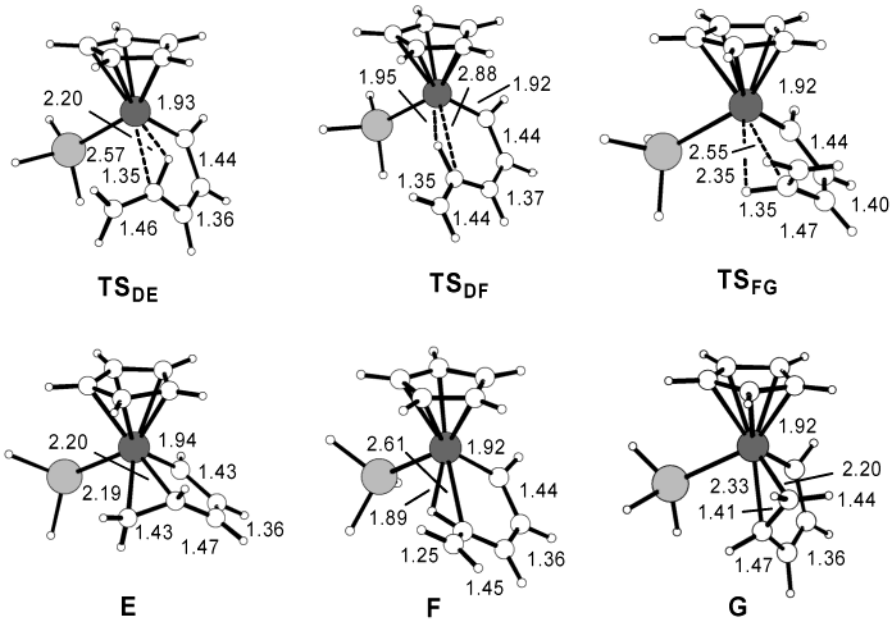

Figure 8. Optimized B3LYP geometries of the equilibrium structures and transition states **E**, **F**, **G**, **TS$_{DE}$**, **TS$_{DF}$**, and **TS$_{FG}$** (distances in Å).

X-ray structures of the related species containing the CpRuBr and RuCp* fragments.[3a,g] GIAO calculations based on the optimum DFT model of **C** give ^{13}C NMR chemical shifts of C_α, C_β, and CH_3 in good agreement with the experimental values of a similar compound (Figure 7). For comparison, the resonances of C_α, C_β, and CH_3 carbon atoms in the $^{13}C\{^1H\}$ NMR spectrum of $[RuCp(=C_2(CH_3)_2C_2(CH_2)_4)(SbPh_3)]^+$ (**2**) give rise to signals at 330.3, 171.3, and 53.5 ppm, respectively. The unusually downfield shifted proton signals of the CH_3 substituent can be interpreted to mean that the C−H bonds are prone to cleavage, in other words, that the hydrogens are rather acidic.

Therefore, **C** may be capable of undergoing a direct 1,2 hydrogen shift to give via **TS$_{CD}$** the intermediate **D**, featuring an agostic C−H bond and still one metal carbon double bond (path **a** in Figure 6). This reaction is endothermic (6.5 kcal/mol) with a comparatively high activation barrier of 35.9 kcal/mol. (Both solvation and tunneling effects[10] may be important in hydrogen shift reactions, which could lower the high activation barrier. Such effects, however, are not taken into account by DFT calculations.) Note further that **TS$_{CD}$** lies closer to **D** than to **C**, since the CH_3−C bond is already short toward a double-bond character. As the reaction proceeds, the CH_3−C bond decreases from 1.50 Å in **C** to 1.40 Å in **TS$_{CD}$** and finally reaches 1.35 Å in **D**, being a typical C=C bond. This is accompanied by migration of a hydrogen atom (essentially a proton) along the π-cloud of the C−C double bond. Thus, the rate-determining step for the formation of butadienyl carbenes is the conversion of **C** to **D**, which is expected to exhibit a large primary kinetic isotope effect. In accordance with the high activation barrier, intermediate **C** could be detected by ^{1}H and ^{13}C NMR spectroscopy even at room temperature and, moreover, a large primary kinetic isotope effect of $k_H/k_D = 10.0$ has been determined. An estimate of the kinetic isotope effect for the conversion of **C** to **D** is provided by the difference in zero-point energies at transition state **TS$_{CD}$** when hydrogen is replaced by deuterium. This estimate gives a value of $k_H/k_D = 10.8$, in excellent agreement with the experimental value.

Also seen in Figure 6, facile rotation about the agostic C−H bond in a clockwise fashion affords eventually via **TS$_{DE}$** the butadienyl carbene **E**, in which the butadienyl moiety adopts a distorted *s-cis* conformation. Alternatively, counterclockwise rotation affords via intermediate **F** the isomeric butadienyl carbene **G**. The rotation barriers are very small, being 2.1, 0.1, and 4.4 kcal/mol for the reaction of **D** to **E**, **D** to **F**, and **F** to **G**, respectively. Since the energy difference between the isomers **E** and **G** is extremely small (only 0.8 kcal/mol), the preference of either **E** or **G** will be guided by the substituents of the alkynes. This is in keeping with experiment (cf. the structures of **3a** and **3c**).

As suggested by a reviewer, an alternative mechanism for the conversion of **C** to butadienyl carbenes may proceed via a C−H activation (β-elimination) route (path **b** in Figure 6) involving species such as **H** and **I**. While from a thermodynamic point of view **H** might be indeed accessible despite the endothermic nature of this reaction (18.1 kcal/mol), kinetically such a process may be rather prohibitive for geometric reasons; that is, the methyl C−H bonds due to the rigid five-membered metallacycle (the Ru−C_α−CH_3 angle in **C** is 126.3°) may be unable to approach the metal center. It has to be noted also that all attempts to locate a transition state for this process failed. It is interesting to note, however, that species **H** is able to undergo facile C−H bond cleavage (β-elimination), requiring only 2.6 kcal/mol to give the hydride η^2-penta-1,3,4-trien-1-yl complex **I**. Unclear is the onward reaction from **I** to eventually yield **E** and/or **G**. In fact, the reductive elimination process to follow might not be easily achieved, requiring severe

(10) For tunneling in hydrogen shift reactions see: Hess, B. A., Jr. *J. Org. Chem.* **2001**, *66*, 5897, and references therein.

rehybridization and rearrangement steps particularly if it is to proceed in an intramolecular fashion.

Conclusion

In this paper we hope to have clarified the ways by which oxidative coupling of alkynes occurs at labile $[RuCp(SbR_3)(CH_3CN)_2]PF_6$. By applying 2,8-decadiyne-d_6 and crossover experiments we could show that the 1,2 hydrogen migration as part of the metallacyclopentatriene−butadienyl carbene transformation takes place in an intramolecular fashion. The large primary kinetic isotope effect points to a direct hydrogen shift (proton migration) without the involvement of hydride species. Furthermore, the various reaction products formed depending on the substituent R′ of the alkyne HC≡CCH$_2$R′ may be useful for further studies.

Experimental Section

General Information. All manipulations were performed under an inert atmosphere of argon by using Schlenk techniques. All chemicals were standard reagent grade and used without further purification. The solvents were purified according to standard procedures.[11] The deuterated solvents were purchased from Aldrich and dried over 4 Å molecular sieves. $[RuCp(SbPh_3)(CH_3CN)_2]PF_6$ (**1a**) and $[RuCp(SbBu^n_3)(CH_3CN)_2]PF_6$ (**1b**) have been prepared according to the literature.[12] The synthesis and characterization of complexes **2**, **3a**−**e**, **5a**, and **5b** have been already reported previously.[2] ^{1}H, ^{2}H, and ^{13}C{^{1}H} NMR spectra were recorded on a Bruker AVANCE-250 spectrometer and were referenced to $SiMe_4$ and benzene-d_6 (set to 7.36 ppm), respectively. ^{1}H and ^{13}C{^{1}H} NMR signal assignments were confirmed by ^{1}H-COSY, DEPT-135, ^{1}H−^{13}C-HSQC, and ^{1}H−^{13}C-HMBCexperiments.

[CpRu(=C$_2$(CD$_3$)C(CH$_2$)$_4$C-η^2-CD=CD$_2$)(SbPh$_3$)]PF$_6$ (3a-d_6). A solution of **1a** (100 mg, 0.134 mmol) in CH_2Cl_2 (5 mL) was treated with 2,8-decadiyne-d_6 (21.9 μL, 0.147 mmol), and the reaction mixture was stirred for 24 h, whereupon the color of the solution turned red. After that the volume of the solution was reduced to about 1 mL, Et_2O was slowly added, and a red microcrystalline precipitate was formed. The supernatant was decanted, and the solid was washed twice with Et_2O and dried under vacuum. Yield: 87 mg (82%). ^{1}H NMR (δ, acetone-d_6, 20 °C): 7.77−7.29 (m, 15H, Ph), 5.56 (s, 5H, Cp), 2.57−1.40 (m, 8H, CH_2). ^{2}H NMR (δ, acetone, 20 °C): 4.89−4.31 (m, 1D, D^a), 3.22−2.73 (m, 1D, D^b), 2.15 (s, 3D, CD_3), 1.47−1.03 (m, 1D, D^b).

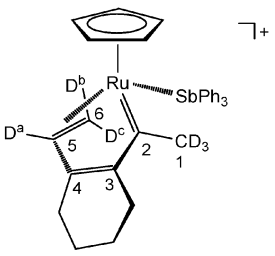

CpRu(−C=CH$_2$)C(CH$_2$)$_4$C-η^2-CH=CH$_2$)(SbPh$_3$) (4). To a solution of **1a** (100 mg, 0.134 mmol) in CH_2Cl_2 (5 mL) was added 1.2 equiv of 2,8-decadiyne (21.9 μL, 0.147 mmol), whereupon the solution turned immediately dark red. After stirring for 24 h, the volume of the solution was reduced to about 1 mL and chromatographed over basic Al_2O_3. The yellow band was collected. After removal of the solvent, the yellow solid was washed with pentane and dried under vacuum. Yield: 59 mg (68%). Anal. Calcd for $C_{33}H_{33}RuSb$: C, 60.75; H, 5.10. Found: C, 60.69; H, 5.14. ^{1}H NMR (δ, CD_2Cl_2, 20 °C): 7.53−7.25 (m, 15H, Ph), 5.46 (d, J_{HH} = 2.4 Hz, 1H, H^b), 4.82 (s, 5H, Cp), 4.79 (d, J_{HH} = 8.9 Hz, 1H, H^d), 4.68 (d, J_{HH} = 2.4 Hz, 1H, H^a), 4.62 (t, J_{HH} = 8.9 Hz, 1H, H^c), 2.73 (d, J_{HH} = 8.9 Hz, 1H, H^e), 2.37−1.05 (m, 8H, CH_2). ^{13}C{^{1}H} NMR (δ, CD_2Cl_2, 20 °C): 161.0 (1C, C^2), 146.4; 146.2 (2C, C^{3,4}), 135.6 (2C, Ph^{2,6}), 134.9 (1C, Ph^1), 129.3 (1C, Ph^1), 128.5 (2C, Ph^{3,5}), 115.4 (1C, C^1), 82.0 (5C, Cp), 62.6 (1C, C^5), 31.5 (1C, C^6), 25.8; 25.6; 23.8; 22.9 (4C, *C*H$_2$).

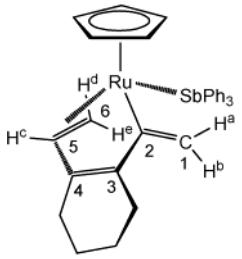

Reaction of 4 with D_2SO_4. A 5 mm NMR tube was charged with **4** (30 mg, 0.046 mmol) in $CDCl_3$ (0.5 mL). Upon addition of D_2SO_4 98% (6.1 μL, 0.115 mmol) the color of the solution changed from yellow to dark red. The reaction was monitored by ^{1}H and ^{13}C NMR spectroscopy, and quantitative formation of **3a**-d_3 was observed. ^{1}H NMR (δ, $CDCl_3$, 20 °C): 7.65−7.03 (m, 15H, Ph), 5.34 (s, 5H, Cp), 5.29 (t, $^3J_{HH}$ = 10.5 Hz, H^a), 3.63 (d, $^3J_{HH}$ = 10.1 Hz, H^b), 2.69−1.18 (m, 8H, C*H*$_2$), 1.71 (d, $^3J_{HH}$ = 10.7 Hz, H^c). ^{13}C{^{1}H} NMR (δ, $CDCl_3$, 20 °C): 334.4 (1C, C^2), 191.4 (1C, C^3), 160.2 (1C, C^4), 135.3 (3C, Ph^{1,2,6}), 131.4 (1C, Ph^4), 130.3 (2C, Ph^{3,5}), 88.2 (5C, Cp), 75.5 (1C, C^5), 50.5−49.0 (m, 1C, C^1), 43.9 (1C, C^6), 36.4; 26.1; 22.2; 22.0; (4C, *C*H$_2$).

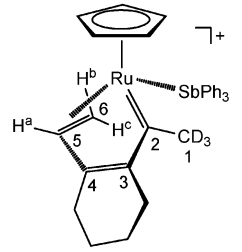

[RuCp(η^3-CH$_2$CCH$_2$−CH=CH-η^1-CO)(SbPh$_3$)]PF$_6$ (6a). A solution of **1a** (140 mg, 0.188 mmol) in 5 mL of CH_2Cl_2 (5 mL) was treated with 2.5 equiv of propargylic alcohol (27.3 μL, 0.469 mmol) and stirred at room temperature for 24 h. After removal of the solvent under reduced pressure, a red-brown solid was obtained, which was purified by column chromatography (neutral Al_2O_3/CH_3NO_2). The red-brown band was collected. Yield: 125 mg (92.0%). Anal. Calcd for $C_{26}H_{26}F_6OPRuSb$: C, 43.24; H, 3.63. Found: C, 43.30; H, 3.57. ^{1}H NMR (δ, acetone-d_6, 20 °C): 7.82−7.09 (m, 15H, Ph), 7.36 (d, J_{HH} = 6.8 Hz, 1H, H^2), 5.81 (s, 5H, Cp), 5.33 (d, J_{HH} = 6.8 Hz, 1H, H^3), 4.27−4.22 (m, 2H ^{H5,6a}), 4,21 (d, J_{HH} = 2.5 Hz, 1H, H^{6s}), 4.02 (d, J_{HH} = 2.5 Hz, 1H, H^{5s}). ^{13}C{^{1}H} NMR (δ, acetone-d_6, 20 °C): 234.6 (1C, *C*O), 150.0 (1C, C^3), 147.8 (1C, C^2), 135.7 (2C, Ph^{2,6}), 135.4 (1C, Ph^1), 131.7 (1C, Ph^4), 130.2 (1C, Ph^{3,5}), 119.4 (1C, C^4), 93.5 (5C, Cp), 68.0 (1C, C^5), 44.5 (1C, C^6). IR (KBr, cm^{-1}): 1688 ($\nu_{C=O}$).

[RuCp(η^3-CH$_2$CCH$_2$-CH=CH-η^1-CO)(SbBu$^n_3$)]PF$_6$ (6b). This complex has been prepared analogously to **6a** with **1b** (300 mg, 0.437 mmol) and propargylic alcohol (55.9 μL, 0.961 mmol) as the starting materials. Yield: 291 mg (96%). Anal. Calcd for $C_{23}H_{38}F_6OPRuSb$: C, 39.56; H, 5.48. Found: C, 39.64; H, 5.54. ^{1}H NMR (δ, acetone-d_6, 20 °C): 7.85 (d, J_{HH} = 6.8 Hz, 1H, H^2), 5.76 (d, J_{HH} = 6.8 Hz, 1H, H^3), 5.73 (s, 5H, Cp), 4.01

(11) Perrin, D. D.; Armarego, W. L. F. *Purification of Laboratory Chemicals*, 3rd ed.; Pergamon: New York, 1988.

(12) Becker, E.; Slugovc, C.; Rüba, E.; Standfest-Hauser, C.; Mereiter, K.; Schmid, R.; Kirchner, K. *J. Organomet. Chem.* **2002**, *649*, 55.

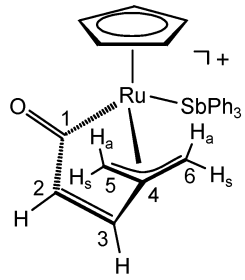

(d, J_{HH} = 3.0 Hz, 1H, H^{6s}), 4.00 (s, 1H, H^{6a}), 3.90 (d, J_{HH} = 3.0 Hz, 1H, H^{5s}), 3.73 (s, 1H, H^{5a}), 2.14−1.94 (m, 6H, Bu), 1.69−1.52 (m, 6H, Bu), 1.49−1.31 (m, 6H, Bu), 0.92 (t, J_{HH} = 7.3 Hz, 9H, CH_3). $^{13}C\{^1H\}$ NMR (δ, acetone-d_6, 20 °C): 235.2 (1C, C^1), 151.1 (1C, C^3), 148.3 (1C, C^2), 117.9 (1C, C^4), 92.2 (5C, Cp), 66.2 (1C, C^5), 42.0 (1C, C^6), 27.6 (3C, CH_2), 25.4 (3C, CH_2), 15.5 (3C, CH_2), 12.7 (3C, CH_3). IR (KBr, cm^{-1}): 1678 ($\nu_{C=O}$).

Calculated ^{1}H and ^{13}C NMR Spectra for [RuCp(η^3-CH_2CCH_2−CH=CH-η^1-CO)($SbMe_3$)]$^+$. ^{1}H NMR: 7.73 (1H, H^2), 5.78 (1H, H^3), 5.38 (5H, Cp), 3.76 (1H, H^{5s}), 3.26 (1H, H^{5a}), 3.24 (1H, H^{6a}), 3.21 (1H, H^{6s}), 0.54 (9H, CH_3). ^{13}C NMR: 234.0 (C^1), 148.0 (C^3), 140.2 (C^2), 118.5 (C^4), 91.3 (Cp, C^7), 71.6 (C^5), 48.2 (C^6), 7.7 (Me).

[CpRu(η^1-CHC(C_6H_9)CH=(η^3-CC$(CH_2)_4$CH)($SbPh_3$)]-PF_6 (7a). To a solution of **1b** (100 mg, 0.134 mmol) in CH_2Cl_2 (5 mL) was added 1-ethynylcyclohexene (31.4 μL, 0.295 mmol), and the reaction mixture was stirred for 2 h at room temperature. After removal of the solvent, the product was collected on a glass frit, washed with Et_2O, and dried under vacuum. Yield: 110 mg (94%). Anal. Calcd for $C_{39}H_{40}F_6PRuSb$: C, 53.44; H, 4.60. Found: C, 53.41; H, 4.64. ^{1}H NMR (δ, acetone-d_6, 20 °C): 8.10 (d, $^4J_{HH}$ = 3.5 Hz, 1H, H^4), 7.57−6.90 (m, 15H, Ph), 6.84 (d, $^4J_{HH}$ = 3.5 Hz, 1H, H^6), 5.90−5.76 (m, 1H, H^8), 5.83 (s, 5H, Cp), 4.10−3.95 (m, 1H, H^1), 3.02−1.19 (m, 16H, CH_2). $^{13}C\{^1H\}$ NMR (δ, acetone-d_6, 20 °C): 197.4 (1C, C^3), 165.5 (1C, C^5), 135.9 (6C, $Ph^{2,6}$), 135.5 (3C, Ph^1), 133.9 (1C, C^4), 133.6 (3C, Ph^4), 130.0 (6C, $Ph^{3,5}$), 124.4 (1C, C^7), 123.9 (1C, C^8), 119.6 (1C, C^6), 94.1 (1C, C^2), 93.0 (5C, Cp), 66.4 (1C, C^1), 29.8−21.3 (8C, CH_2).

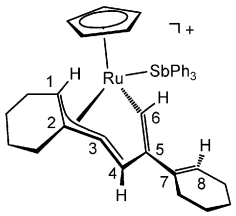

[CpRu(η^1-CHC(C_6H_9)CH=(η^3-CC$(CH_2)_4$CH)($SbBu^n_3$)]-PF_6 (7b). This complex has been prepared analogously to **7a** with **1b** (100 mg, 0.146 mmol) and 1-ethynyl cyclohexene (37.6 μL, 0.321 mmol) as the starting materials. Yield: 108 mg (91%). Anal. Calcd for $C_{33}H_{52}F_6PRuSb$: C, 48.54; H, 6.42. Found: C, 48.49; H, 6.37. ^{1}H NMR (δ, acetone-d_6, 20 °C): 8.13 (d, $^4J_{HH}$ = 3.4 Hz, 1H, H^4), 7.11 (d, $^4J_{HH}$ = 3.4 Hz, 1H, H^6), 6.02−5.94 (m, 1H, H^8), 5.65 (s, 5H, Cp), 3.72 (d, $^3J_{HH}$ = 6.9 Hz, 1H, H^1), 3.40−1.47 (m, 28H, CH_2), 1.36 (q, $^3J_{HH}$ = 7.3 Hz, 6H, CH_2), 0.89 (t, $^3J_{HH}$ = 7.3 Hz, 9H, CH_3). $^{13}C\{^1H\}$ NMR (δ, acetone-d_6, 20 °C): 197.5 (1C, C^3), 162.3 (1C, C^5), 136.4 (1C, C^4), 135.3 (1C, C^7), 123.6 (1C, C^8), 118.3 (1C, C^6), 92.8 (5C, Cp), 91.4 (1C, C^2), 61.8 (1C, C^1), 29.0−14.1 (17C, CH_2), 13.6 (3C, CH_3).

[(RuCp(η^1-CHC(C_6H_{10}OH)CH=(η^3-CC$(CH_2)_4$CH)-($SbBu^n_3$)]PF_6 (8). This complex has been prepared analogously to **7a** with **1b** (100 mg, 0.146 mmol) and 1-ethynylcyclohexanol (40 mg, 0.161 mmol) as the starting materials. Yield: 85 mg (71%). Anal. Calcd for $C_{33}H_{54}F_6OPRuSb$: C, 47.49; H, 6.52. Found: C, 49.47; H, 6.59. ^{1}H NMR (δ, acetone-d_6, 20 °C): 8.14 (d, J_{HH} = 3.4 Hz, 1H, H^4), 6.95 (d, J_{HH} = 3.4 Hz, 1H, H^6), 5.60 (s, 5H, Cp), 3.71 (d, J_{HH} = 6.8 Hz, 1H, H^1), 3.51 (s, 1H, OH), 3.31 (td, $^1J_{HH}$ = 17.7 Hz, $^2J_{HH}$ = 6.8 Hz, 1H, CH_2), 2.98−1.16 (m, 35H, CH_2), 0.90 (t, J_{HH} = 7.2 Hz, 9H, CH_3). $^{13}C\{^1H\}$ NMR (δ, acetone-d_6, 20 °C): 197.8 (1C, C^3), 171.7 (1C, C^5), 134.0 (1C, C^4), 119.0 (1C, C^6), 91.9 (5C, Cp), 90.6 (1C, C^2), 73.2 (1C, C^7), 37.8; 37.8; 29.6; 27.4; 25.5; 22.0; 21.9; 21.7; 21.1 (9C, CH_2), 28.3; 25.6; 13.0 (9C, CH_2), 12.8 (3C, CH_3).

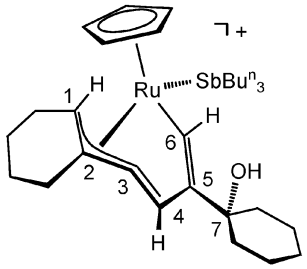

[RuCp(η^1-CHC$(Me)_2$OHCH=(η^3-CC$(Me)CH_2$)(SbR_3)]-PF_6 (9). This complex has been prepared analogously to **7a** with **1b** (300 mg, 0.437 mmol) and 2-methylbut-3-yn-2-ol (93.2 μL, 2.885 mmol) as the starting materials. The crude product was purified by column chromatography (neutral Al_2O_3/CH_2Cl_2/acetone). Yield: 245 mg (76%). Anal. Calcd for $C_{27}H_{46}F_6OPRuSb$: C, 42.99; H, 6.15. Found: C, 42.89; H, 6.25. ^{1}H NMR (δ, acetone-d_6, 20 °C): 8.22 (d, J_{HH} = 3.4 Hz, 1H, H^4), 7.00 (d, J_{HH} = 3.4 Hz, 1H, H^6), 5.66 (s, 5H, Cp), 3.79 (s, 1H, OH), 3.41 (d, J_{HH} = 1.1 Hz, 1H, H^1), 2.42 (s, 3H, CH_3), 2.34 (d, J_{HH} = 1.1 Hz, 1H, H^1), 1.43 (s, 3H, CH_3), 1.42 (s, 3H, CH_3), 1.90−1.78 (m, 6H, CH_2), 1.64−1.48 (m, 6H, CH_2), 1.43−1.32 (m, 6H, CH_2), 0.90 (t, J_{HH} = 7.3 Hz, 9H, CH_3). $^{13}C\{^1H\}$ NMR (δ, acetone-d_6, 20 °C): 199.5 (1C, C^3), 171.9 (1C, C^5), 133.5 (1C, C^4), 117.9 (1C, C^6), 90.7 (5C, Cp), 83.8 (1C, C^2), 68.9 (1C, C^7), 32.9 (1C, C^1), 30.2; 30.1 (2C, CH_3), 28.1; 25.6 (6C, CH_2), 22.7 (1C, CH_3),-13.2 (3C, CH_2),12.8 (3C, CH_3).

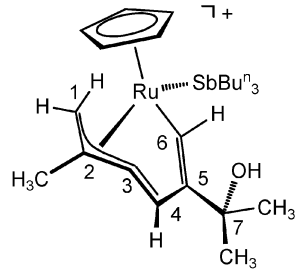

Computational Details. All calculations were performed using the Gaussian98 software package on the Silicon Graphics Origin 2000 of the Vienna University of Technology.[13] The geometry and energy of the model complexes and the transition states were optimized at the B3LYP level[14] with the Stuttgart/

(13) Frisch, M. J.; Trucks, G. W.; Schlegel, H. B.; Scuseria, G. E.; Robb, M. A.; Cheeseman, J. R.; Zakrzewski, V. G.; Montgomery, J. A., Jr.; Stratmann, R. E.; Burant, J. C.; Dapprich, S.; Millam, J. M.; Daniels, A. D.; Kudin, K. N.; Strain, M. C.; Farkas, O.; Tomasi, J.; Barone, V.; Cossi, M.; Cammi, R.; Mennucci, B.; Pomelli, C.; Adamo, C.; Clifford, S.; Ochterski, J.; Petersson, G. A.; Ayala, P. Y.; Cui, Q.; Morokuma, K.; Malick, D. K.; Rabuck, A. D.; Raghavachari, K.; Foresman, J. B.; Cioslowski, J.; Ortiz, J. V.; Stefanov, B. B.; Liu, G.; Liashenko, A.; Piskorz, P.; Komaromi, I.; Gomperts, R.; Martin, R. L.; Fox, D. J.; Keith, T.; Al-Laham, M. A.; Peng, C. Y.; Nanayakkara, A.; Gonzalez, C.; Challacombe, M.; Gill, P. M. W.; Johnson, B. G.; Chen, W.; Wong, M. W.; Andres, J. L.; Head-Gordon, M.; Replogle, E. S.; Pople, J. A. *Gaussian 98*, revision A.7; Gaussian, Inc.: Pittsburgh, PA, 1998.

(14) (a) Becke, A. D. *J. Chem. Phys.* **1993**, *98*, 5648. Miehlich, B.; Savin, A.; Stoll, H.; Preuss, H. *Chem. Phys. Lett.* **1989**, *157*, 200. (b) Lee, C.; Yang, W.; Parr, G. *Phys. Rev. B* **1988**, *37*, 785.

Table 1. Details for the Crystal Structure Determinations of Complexes 4, 3c, 5a·$(CH_3)_2CO$, and 5a′

	4	**3c**	**5a·$(CH_3)_2CO$**	**5a′**
formula	$C_{33}H_{33}RuSb$	$C_{35}H_{40}F_6PRuSb$	$C_{44}H_{42}F_6OPRuSb$	$C_{41}H_{36}F_6PRuSb$
fw	652.41	828.46	954.57	896.49
cryst size, mm	0.14 × 0.12 × 0.10	0.80 × 0.40 × 0.08	0.60 × 0.40 × 0.02	0.72 × 0.18 × 0.11
space group	$P2_1/c$ (No. 14)	$P2_1/n$ (No. 14)	$P2_1/n$ (No. 14)	$P2_1/n$ (No. 14)
a, Å	9.796(3)	11.459(3)	14.081(6)	13.382(4)
b, Å	15.368(5)	20.681(5)	12.488(5)	18.470(6)
c, Å	18.601(6)	14.668(4)	24.055(9)	14.760(5)
β, deg	101.82(1)	90.86(2)	99.52(1)	98.01(2)
V, Å^3	2741(2)	3476(2)	4172(3)	3613(2)
Z	4	4	4	4
ρ_{calc}, g cm^{-3}	1.581	1.583	1.520	1.648
T, K	297 (2)	223(2)	297(2)	223(2)
μ, mm^{-1} (Mo Kα)	1.556	1.313	1.107	1.270
F(000)	1304	1656	1912	1784
abs corr	multiscan	multiscan	multiscan	multiscan
θ_{max}, deg	27	25	30	27
no. of reflns measd	24 251	35 096	10 425	41 666
no. of unique reflns	5973	6042	6801	7863
no. of rflns $I > 2\sigma(I)$	3931	9168	3560	6224
no. of params	331	397	487	454
R_1 ($I > 2\sigma(I)$)[a]	0.035	0.049	0.056	0.038
R_1 (all data)	0.074	0.065	0.124	0.055
wR_2 (all data)	0.075	0.119	0.150	0.110
diff Four. peaks min/max, e Å^{-3}	−0.56/1.15	−0.93/1.46	−0.82/0.79	−0.83/1.53

[a] $R_1 = \sum||F_o| - ||F_c||/\sum|F_o|$, $wR_2 = [\sum(w(F_o^2 - F_c^2)^2)/\sum(w(F_o^2)^2)]^{1/2}$.

Dresden ECP (SDD) basis set[15] to describe the electrons of the Ru and Sb atoms. For the H and C atoms the 6-31g** basis set was employed.[16] A vibrational analysis was performed to confirm that the structures of the model compounds have no imaginary frequency. The transition state structure was relaxed after applying a small perturbation to ensure that it is connected to the corresponding reactant and product. A vibrational analysis was also performed to confirm that it has only one imaginary frequency. The geometries were optimized without constraints (C_1 symmetry). ^{1}H and ^{13}C chemical sifts were calculated at the B3LYP level of theory for the optimized structure of $[RuCp(\eta^3\text{-}CH_2CCH_2{-}CH{=}CH\text{-}\eta^1\text{-}CO)(SbMe_3)]^+$ using the gauge-independent atomic orbital (GIAO) method in Gaussian 98 with the above basis sets. Chemical shifts are given with respect to $Si(Me_3)_4$ (TMS) at the same computational level.

X-ray Structure Determination for 4, 3c, 5a·$(CH_3)_2CO$, and 5a′. Crystals of **4** were obtained by diffusion of pentane into a CH_2Cl_2 solution, whereas crystals of **3c**, **5a**·$(CH_3)_2CO$, and **5a′** were obtained by diffusion of Et_2O into acetone or CH_2Cl_2 solutions. Crystal data and experimental details are given in Table 1. X-ray data were collected on a Bruker Smart CCD area detector diffractometer (graphite-monochromated Mo Kα radiation, $\lambda = 0.71073$ Å, 0.3° ω-scan frames). Corrections for Lorentz and polarization effects, for crystal decay, and for absorption were applied.[17] The structures were solved by direct methods using the program SHELXS97.[18] Structure refinement on F^2 was carried out with program SHELXL97.[18] All non-hydrogen atoms were refined anisotropically. Most hydrogen atoms were inserted in idealized positions and were refined riding with the atoms to which they were bonded. Some crucial hydrogen atoms were refined in x, y, and z using only C−H distance restraints.

Acknowledgment. Financial support by the "Fonds zur Förderung der Wissenschaftlichen Forschung" (Project No. P14681-CHE) is gratefully acknowledged.

Supporting Information Available: Listings of atomic coordinates, anisotropic temperature factors, and bond lengths and angles for **4**, **3c**, **5a**·$(CH_3)_2CO$, and **5a′**. This material is available free of charge via the Internet at http://pubs.acs.org.

OM030039N

(15) (a) Haeusermann, U.; Dolg, M.; Stoll, H.; Preuss, H. *Mol. Phys.* **1993**, *78*, 1211. (b) Kuechle, W.; Dolg, M.; Stoll, H.; Preuss, H. *J. Chem. Phys.* **1994**, *100*, 7535. (c) Leininger, T.; Nicklass, A.; Stoll, H.; Dolg, M.; Schwerdtfeger, P. *J. Chem. Phys.* **1996**, *105*, 1052.

(16) (a) McClean, A. D.; Chandler, G. S. *J. Chem. Phys.* **1980**, *72*, 5639. (b) Krishnan, R.; Binkley, J. S.; Seeger, R.; Pople, J. A. *J. Chem. Phys.* **1980**, *72*, 650. (c) Wachters, A. J. H. *J. Chem. Phys.* **1970**, *52*, 1033. (d) Hay, P. J. *J. Chem. Phys.* **1977**, *66*, 4377. (e) Raghavachari, K.; Trucks, G. W. *J. Chem. Phys.* **1989**, *91*, 1062. (f) Binning, R. C.; Curtiss, L. A. *J. Comput. Chem.* **1995**, *103*, 6104. (g) McGrath, M. P.; Radom, L. *J. Chem. Phys.* **1991**, *94*, 511.

(17) *Bruker, Programs SMART*, version 5.054; *SAINT*, version 6.2.9; *SADABS*, version 2.03; *XPREP*, version 5.1; *SHELXTL*, version 5.1; Bruker AXS Inc.: Madison, WI, 2001.

(18) Sheldrick, G. M. *SHELX97*, Program System for Crystal Structure Determination; University of Göttingen: Germany, 1997.